IEEE Access
Multidisciplinary | Rapid Review | Open Access Journal

Received March 18, 2020, accepted April 6, 2020, date of publication April 16, 2020, date of current version May 1, 2020.

Digital Object Identifier 10.1109/ACCESS.2020.2988348

A Low-Cost, Portable Solution for Stress and Relaxation Estimation Based on a Real-Time Fuzzy Algorithm

UNAI ZALABARRIA, ELOY IRIGOYEN, (Member, IEEE), RAQUEL MARTINEZ, MIKEL LARREA, AND ASIER SALAZAR-RAMIREZ

Department of Systems Engineering and Automation, Faculty of Engineering, University of the Basque Country (UPV/EHU), 48013 Bilbao, Spain

Corresponding author: Unai Zalabarria (unai.zalabarria@ehu.eus)

This work was supported in part by the ERDF/Spanish Ministry of Science, Innovation and Universities, National Research Agency/PhysComp Project under Grant TIN2017-85409-P.

ABSTRACT *Goal*: This paper proposes a reliable stress and relaxation level estimation algorithm that is implemented in a portable, low-cost hardware device and executed in real time. The main objective of this work is to offer an affordable and "ready-to-go" solution for medical and personal environments, in which the detection of the arousal level of a person is crucial. *Methods*: To achieve meaningful identification of stress and relaxation, a fuzzy algorithm based on expert knowledge is built according to parameters extracted from physiological records. In addition to the heart rate, parameters extracted from the galvanic skin response and breath are employed to extend the results. Moreover, this algorithm achieves accurate results with a restricted computational load and can be implemented in a miniaturized low-cost prototype. The developed solution includes standard and actively shielded electrodes that are connected to an Arduino device for acquisition, while parameter extraction and fuzzy processing are conducted with a more powerful Raspberry Pi board. The proposed solution is validated using real physiological registers from 42 subjects collected using BIOPAC MP36 hardware. Additionally, a real-time acquisition, processing and remote cloud storage service is integrated via IoT wireless technology. *Results*: Robust identification of stress and relaxation is achieved, with F1 scores of 91.15% and 96.61%, respectively. Moreover, processing is performed using a 20-second sliding window; thus, only a small frame of context is required. *Significance*: This work presents a reliable solution for identifying stress and relaxation levels in real time, which can lead to the production of low-cost commercial devices for use in medical and personal environments.

INDEX TERMS Stress, relaxation, physiology, fuzzy logic, Internet of Things.

I. INTRODUCTION

In the literature, stress is defined as the natural response of an organism in any situation, regardless of whether this response is negative or positive. The organism responds by activation of the sympathetic nervous system, which causes a psychophysiological change. This process allows the body to adapt to a situation by either facing the situation or remaining in a state of energy conservation [1]–[3]. Conversely, relaxation deactivates the autonomous nervous system (ANS) via the action of the parasympathetic nervous system once the stressful situation has concluded. The study of the body response in this deactivation phase is interesting since understanding the pathway of relaxation can provide information about specific pathologies or applications [4], [5].

Stress and relaxation processes are parts of everyday life and are a growing concern for society, especially when the impact on health is negative [2], [6], [7]. According to a statement from the European Commission in 2017, work-related stress is one of the most challenging and growing occupational safety and health concerns. Over half of EU workers report that stress is common in their workplaces, and 4 of 10 workers think that their stress is not handled well [8].

The pace of modern life causes many people to suffer from continuous stress; this condition is also known as distress. This aversive state reduces work efficiency and causes negative emotions and various illnesses [2], [6]. Stress can cause various diseases, including chronic illnesses (e.g.,

The associate editor coordinating the review of this manuscript and approving it for publication was Muhammad Imran Tariq.

cardiovascular diseases, diabetes, and some forms of cancer) and can increase social costs, especially in developed countries [3], [4], [7]. Considering the new paradigms of positive psychology, many research lines have shifted focus in this area to seeking solutions that are centered on wellness and analyzing how people relax [5], [9].

The detection, identification and classification of these processes is a challenging problem that needs new proposals based on portable solutions. The main drawbacks of current monitoring devices are their high costs. These costs put technology out of reach for many people and medical centers.

Among the existing proposals, Gjoreski *et al.* [10] used a wrist device to perform stress detection with 70% sensitivity from photoplethysmogram (PPG), galvanic skin response (GSR), skin temperature (ST) and acceleration registers (ACC). They utilized 2-minute intervals and 20-minute intervals for short-term-based stress detection and context-based stress detection, respectively. Han *et al.* [6] performed stress detection from electrocardiogram (ECG) and breathing (RSP) records acquired at 1-minute intervals using a wearable device; however, these records are processed offline after acquisition is finished. Golgouneh and Tarvirdizadeh [11] proposed an online stress detection algorithm that is implemented in a portable device. They achieve 81% accuracy processing PPG and GSR registers at 20-second intervals. Minguillon *et al.* [12] presented a portable real-time stress detection device that consists of multiple biosignal sensors (ECG, GSR, electroencephalogram (EEG) and electromyogram (EMG)), the RaBio w8 system, a laptop and an Arduino e-Health board. They achieved 86% accuracy using a 2-second interval. Salai *et al.* [13] integrated a stress detection algorithm in a low-cost portable device and achieved 74.6% accuracy by analyzing 560 RR intervals extracted from ECG. These works are listed in Table 5 of Section III as comparative references to support the results obtained in this study.

The recent popularity of the IoT paradigm has caused an increase in the amount of information that is stored in medical databases [14]–[16]. This approach makes patient information available anywhere and anytime from either a computer or a mobile device (after the corresponding ethical and confidentiality approvals) [16].

This paper presents a high-accuracy real-time stress and relaxation level estimation algorithm that is implemented on a low-cost portable device. The proposed method estimates stress and relaxation by applying expert knowledge via rules in a fuzzy logic algorithm that processes parameters extracted from ECG, GSR and RSP in a 20-second sliding window. The algorithm has been tested to ensure that the hardware can perform concurrently in real time. This work also proposes the use of the differential area between the GSR signal and its first-order interpolation as a substitute for raw GSR to avoid differences in thresholds for different subjects during the same stress situations. The results obtained in the proposal presented in [17] are improved by adding the standard deviation of the RSP frequencies, which is calculated using a fast Fourier transform of reduced size to avoid excessive energy consumption due to its relatively high computational load.

Several approaches were studied to produce a solution that combines a low-cost platform with wireless implementation [18]–[21]. Considering size, popularity and price, Arduino Micro (18€) and Raspberry Pi Zero (20€) devices have proven to be suitable for a robust and low-cost prototype [14]–[17]. Both platforms were combined to obtain a miniaturized solution: Arduino Micro for real-time physiological data acquisition and Raspberry Pi Zero for running the developed algorithms. In addition, a secure cloud storage solution is proposed to enable remote access to the information.

This paper is organized as follows: Section II focuses on the proposed methodology. In Section III, the results are presented and discussed. Section IV describes the conclusions.

II. METHOD

This section is divided into three well-defined stages. The first stage is the experimental stage, in which the process of obtaining physiological records is explained. The second stage introduces the developed software and describes the implemented processing techniques and fuzzy algorithm used to estimate the stress and relaxation levels. The third stage addresses the implementation of the developed algorithm into a hardware prototype.

A. EXPERIMENTAL STAGE

In this work, a particular experimental stage was designed to obtain physiological records based on that previously established by authors, including Gross and Levenson [22] and Martinez *et al.* [23]. Experimental protocols often utilize film clips to induce emotions [22], followed by personalized recall, real-life experiences and picture viewing [24]. Music, which decreases anxiety and reduces both blood pressure and heart rate in stressful situations, is also used to restore basal psychological and physiological functioning [25]. This experiment consists of a three-phase challenge with an approximate duration of 14 minutes; the experiment is outlined in Figure 1. In the first and third phases, the person is taken to a basal state of relaxation using relaxing videos and music. In the second phase, stress is induced by asking the person to perform a three-dimensional puzzle.

To achieve a reliable dataset of physiological records for software validation, a standard medical device with its corresponding professional electrodes was employed. The data were collected using BIOPAC MP36 hardware (Biopac Systems Inc., USA) at a 1000-Hz sampling rate and Acq-Knowledge 3.7.1 software. The acquired records were also employed in Subsection II-C.4 during hardware validation to simulate the analog input using a methodology that is referred to as ''Human in the loop''.

A total of 42 participants (31 male and 11 female) between 19 and 45 years of age (mean = 22.88; SD = 3.1) participated in the experiment in 2014. All subjects were volunteers of the engineering school at the University of the Basque Country

FIGURE 1. Phases and durations of the experimental stages for the acquisition of physiological records.

(UPV/EHU). In addition, the design and implementation of the experiment was reviewed and certified by the ethical committee of the UPV/EHU, more specifically, by CEISH-UPV/EHU, BOPV 32 (M10_2016_189) [26]. Subsequently, these data were partially labeled as stress and relaxation by UPV/EHU physiology experts for validation purposes.

Although each participant has different stress and relaxation thresholds, they all respond to both situations to some extent. In Subsection II-B.2, a physiological parameter normalization is carried out to standardize the physiological responses obtained in the different phases of the experiment.

Considering the importance of some physiological signals in the estimation of stress and relaxation, heart period (HP), GSR and RSP were monitored using noninvasive sensors [10], [17], [20], [21], [27], [28]. Figure 2 shows the placement of the sensors that are utilized to collect these signals with the BIOPAC MP36 hardware.

The method employed for the acquisition of each of the signals, in addition to its relationship with the stress and relaxation states, is detailed as follows:

Heart Period: Since the HP cannot be obtained directly by sensors, determining the most appropriate practice for this context is necessary. ECG and PPG are the most popular signals, from which the heart period is derived. A comparative review of PPG against ECG stated that PPG can be applied during rest but not during stress [29]. Stress changes the elasticity of the arteries, inducing variations in pulse transit and, consequently, modifying the interbeat interval [30], [31]. Thus, ECG is more appropriate for extracting HP in stress and relaxation conditions. The ECG signal was collected using an "Einthoven's triangle" configuration, as it is a popular method for noninvasive sensorization [4]. The movements of a person and electromagnetic interference induce several artifacts in ECG, which increases the difficulty of HP extraction. Therefore, the algorithm developed in [32] was employed to perform robust detection of R-peaks, from which the HP is calculated according to the equation (1).

$$HP_i = rpeak_i - rpeak_{i-1} \tag{1}$$

where $rpeak_i$ is the i^{th} R-peak's temporal location expressed in seconds.

Galvanic Skin Response: GSR measured in palmar glands is highly correlated with sympathetic action [4]. One of the most common electrode placements for acquiring GSR signals is the medial phalanges of the fingers. In this work, the nondominant hand is used, leaving the other hand free to perform the tasks of the experiment.

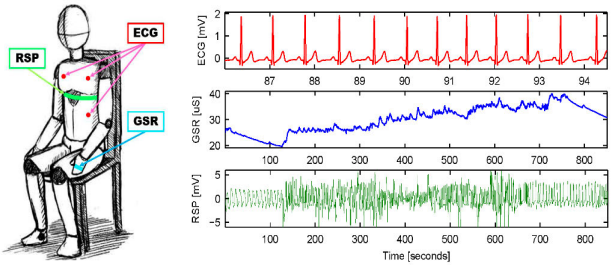

FIGURE 2. Electrode positioning scheme and collected registers.

Breathing: Cardiovascular measures are modulated by respiratory effects, which are important in the interpretation of ANS functioning [4], [24]. An impedance band is used to measure this signal; thus, it is possible to visualize the expansion and contraction of the chest.

B. SOFTWARE DEVELOPMENT

Physiological changes due to stress and relaxation can be detected by sensors that measure the physiological responses elicited by the ANS. Hence, the level of arousal or activation of the sympathetic and parasympathetic nervous systems can be calculated [2], [4], [24].

To achieve this goal, the first phase of parameter extraction was performed. The parameters are closely related to changes in the ANS. Thus, patterns that indicate the activation of stress and relaxation states can be detected. Subsequently, these patterns were modeled in the second phase of parameter extraction, in which a fuzzy logic model was applied to estimate the stress and relaxation level by applying expert knowledge via well-defined rules [17], [27], [33].

1) EXTRACTION OF RELEVANT PARAMETERS

To extract complementary information about ANS functioning, a comprehensive assessment of cardiovascular, electrodermal, and respiratory measures was performed [2], [4], [24]. A total of 5 physiological parameters were extracted: mean HP, variation in the HP, variation in the GSR, differential area between the GSR and its first-order interpolation and the product between the root mean square of HP and the standard deviation of the frequency correlation of the RSP. These parameters are closely related to stress and relaxation

events, as demonstrated in previous works [2], [4], [17], [23], [24], [27], [34].

The extraction was performed using a 20-second sliding window, which is sufficient for performing robust parameter extraction and real-time processing, as established in previous works [17], [27], [32].

a: MEAN HEART PERIOD (MHP)

is defined as the mean HP according to formula (2), where N_1 is the *HP* length. This parameter is of great interest due to the influence of both the sympathetic and parasympathetic branches of the ANS [4].

$$MHP = \frac{\sum_{i=1}^{N_1} HP_i}{N_1} \tag{2}$$

b: THE VARIATION IN THE HEART PERIOD (VHP)

is obtained by extracting the slope from the first-order interpolation of the HP values. VHP represents the changes in the balance between the sympathetic and parasympathetic nervous systems [4]. The slope is extracted via linear regression according to formula (3).

$$VHP = \frac{\sum_{i=1}^{N_1} rpeak_i HP_i - \frac{\sum_{j=1}^{N_1+1} rpeak_j \sum_{i=1}^{N_1} HP_i}{N_1}}{\sum_{i=1}^{N_1} rpeak_i^2 - \frac{(\sum_{j=1}^{N_1+1} rpeak_j)^2}{N_1}} \tag{3}$$

Positive and negative values in the ***variation in the galvanic skin response (VGSR)*** correspond to activation and deactivation, respectively, of the sympathetic nervous system [2], [4], [24]. This phenomenon is clearly represented in Figure 3. To quantify the VGSR, the slope of the GSR first-order interpolation is extracted according to formula (4), where $time_i$ corresponds to the i^{th} GSR's temporal location expressed in seconds and N_2 is the *GSR* length.

$$VGSR = \frac{\sum_{i=1}^{N_2} time_i GSR_i - \frac{\sum_{i=1}^{N_2} time_i \sum_{i=1}^{N_2} GSR_i}{N_2}}{\sum_{i=1}^{N_2} time_i^2 - \frac{(\sum_{i=1}^{N_2} time_i)^2}{N_2}} \tag{4}$$

The GSR values tend to be more chaotic during stressful periods, whereas in relaxed states, the signal stabilizes and resembles a straight line with a constant slope [23], [34]. In this work, this characteristic was collected by measuring the ***differential area between the GSR signal and its first-order interpolation (AGSR)***, as shown in Figure 3. A greater value of this parameter implies that the GSR signal is more distinct from a straight line. AGSR is calculated according to formula (6), where *offset* is the value required to place the interpolation in the correct position of the vertical axis, which conforms to equation (5).

$$offset = \frac{\sum_{i=1}^{N_2} GSR_i - VGSR \cdot \sum_{i=1}^{N_2} time_i}{N_2} \tag{5}$$

$$AGSR = \frac{\sum_{i=1}^{N_2} \mid GSR_i - (offset + VGSR_i \cdot time_i) \mid}{N_2} \tag{6}$$

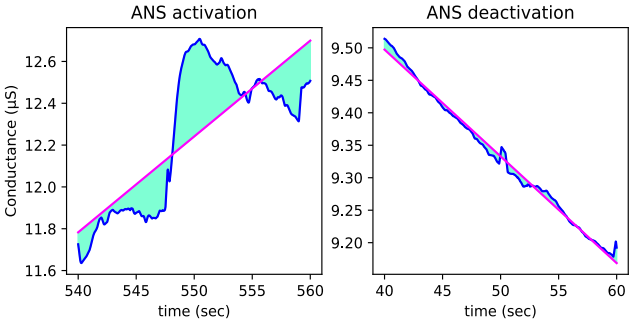

FIGURE 3. The light blue zone represents the differential area between the GSR signal (blue) and the approximate first-order function (pink). The value of the AGSR increases as the GSR becomes more chaotic during ANS activation.

During relaxation, respiratory sinus arrhythmia is frequently employed as an index of cardiac vagal tone [35]. This feature represents the contribution of the parasympathetic nervous system to cardiac regulation [4], [31]. However, in stressful situations, the breath becomes more frequent and inharmonious [23], [27], [36]. These changes are noticeable in Figure 4, where the spectral representation of the signal is calculated via a fast Fourier transform (7). The standard deviation of the frequencies (SDCC) is calculated according to formula (8), which is correlated with stress and relaxation events. Due to the similarity of this parameter with the root mean square of HP (RMS) calculated in (9), the combination of the SDCC and RMS produced a more reliable representation of the stress and relaxation levels, as indicated by the calculation of the ***product between RMS and SDCC (HSCR)***, which conforms to formula (10). Figure 5 shows an example of RMS and SDCC under stress and relaxation and the enhanced HSCR.

$$fft_k = \sum_{n=1}^{N_3} RSP_n \cdot e^{-j2\pi k \frac{n-1}{N_3}} \tag{7}$$

$$SDCC = \sqrt{\frac{\sum_{k=1}^{N_4} (fft_k - \overline{fft})^2}{N_4}} \tag{8}$$

$$RMS = \sqrt{\frac{\sum_{i=1}^{N_1} HP_i^2}{N_1}} \tag{9}$$

$$HSCR = SDCC \cdot RMS \tag{10}$$

where N_3 and N_4 refer to the length of the *RSP* and the number of spectral lines of the *fft* respectively.

2) PARAMETER NORMALIZATION

Parameter values may vary among subjects in identical stress and relaxation situations. Thus, absolute values cannot be applied to estimate whether the subject is relaxed or stressed. To solve this problem, parameter normalization is implemented so that each range of values has the same interpretation for every subject. The formulas applied to normalize MHP (11), VHP (12), VGSR (13), AGSR (14) and HSCR

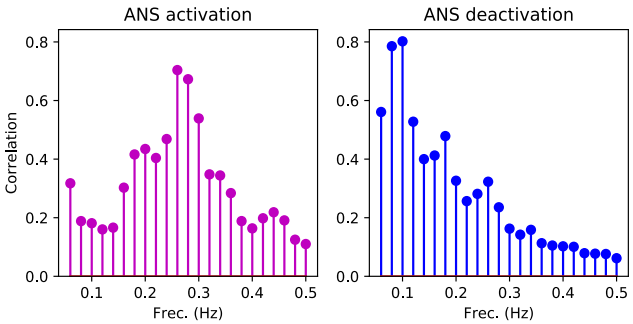

FIGURE 4. Spectral analysis of the RSP signal. The graph on the left belongs to the stress phase, and the one on the right belongs to the relaxation phase.

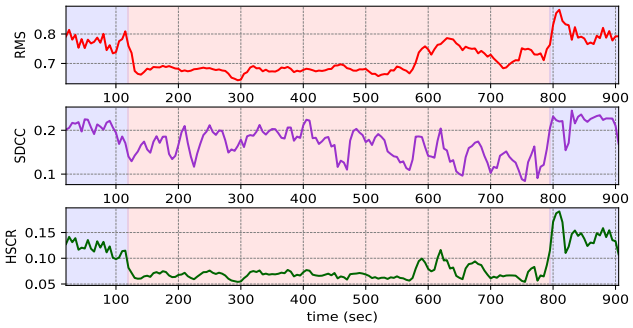

FIGURE 5. Product between RMS (first graph) and SDCC (second graph) resulting in HSCR (third graph), which represents a robust expression of stress and relaxation.

(15) are shown here.

$$MHP_{norm} = \frac{MHP - min(MHP)}{max(MHP) - min(MHP)} \tag{11}$$

$$VHP_{norm} = \frac{VHP}{std(VHP)} \tag{12}$$

$$VGSR_{norm} = \frac{VGSR}{std(VGSR)} \tag{13}$$

$$AGSR_{norm} = \frac{AGSR - min(AGSR)}{median(AGSR - min(AGSR))} \tag{14}$$

$$HSCR_{norm} = \frac{HSCR - min(HSCR)}{max(HSCR) - min(HSCR)} \tag{15}$$

3) FUZZY ALGORITHM CONFIGURATION

A rule-based fuzzy logic algorithm is implemented to combine the previously normalized parameters for stress and relaxation level estimation. The output ranges from 0 to 1, where 0 represents the maximum relaxation level and 1 represents the maximum stress level. Table 1 shows the configuration that is employed to set up the membership function (MF) for each input and output, where SMF, PIMF, ZMF and TRAPMF refer to the S-shaped MF, Pi-shaped MF, Z-shaped MF and trapezoidal MF, respectively. Expert knowledge is applied via well-defined rules extracted from the literature [1], [2], [4], [23], [24], [31]. This approach facilitated construction of the rule set shown in Table 2.

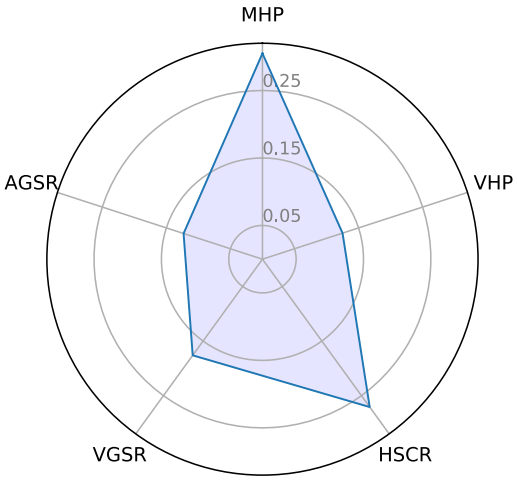

FIGURE 6. Total weighting of each parameter in the rule set.

Figure 6 shows the total weight of each parameter in the rule set. MHP and HSCR are the parameters with greater weight because both parameters are derived from the cardiovascular response; thus, they are strongly correlated with both the sympathetic activity and the parasympathetic activity of the autonomic nervous system. Conversely, the parameters derived from the GSR are closely related to sympathetic activity, which renders them suitable for measuring the activity of the sympathetic nervous system but unsuitable for that of the parasympathetic [4].

C. HARDWARE IMPLEMENTATION

The prototype developed in this work was built by combining three low-cost devices, each of which is employed for a different stage of the system. First, an Arduino Micro (ArdM) board was utilized for analog acquisition of physiological records. Second, a Raspberry Pi Zero (RPiZ) board was configured to perform parameter extraction, normalization and fuzzy processing. Last, a server was implemented in a standard PC to store the results received from the RPiZ. In addition, a National Instruments board was employed to reproduce the physiological signals that were previously acquired with the BIOPAC MP36 device. This methodology, which is referred to as "human in the loop" by the authors, benefits from using real signals as if a person was connected to the system and avoids the risks and difficulties of experimentation with humans. This methodology will be further explained in Subsection II-C.4. Figure 7 shows a schematic representation of the devices with the corresponding interconnections.

1) ACQUISITION

Due to its small size, low cost and potential for acquiring analog data in real time, the ArdM platform is considered an optimal solution for acquiring physiological data [14]–[16]. The programming has been carried out in the Arduino

TABLE 1. Implemented membership function parameters.

Type	Name	Range	MF name	MF type	MF parameters
Input 1	MHP	[0 1]	Low	SMF	[0.5 1]
			Medium	PIMF	[0 0.5 0.5 1]
			High	ZMF	[0 0.5]
Input 2	VHP	[-2 2]	Low	SMF	[0 1.5]
			Medium	PIMF	[-1.5 0 0 1.5]
			High	ZMF	[-1.5 0]
Input 3	VGSR	[-2 2.5]	Low	ZMF	[-2 0]
			Medium	PIMF	[-2 0 0 2.5]
			High	SMF	[0 2.5]
Input 4	AGSR	[0 1]	Low	ZMF	[0 1]
			High	SMF	[0 1]
Input 5	HSCR	[0 1]	Low	SMF	[0.5 1]
			Medium	PIMF	[0 0.5 0.5 1]
			High	ZMF	[0 0.5]
Output	Stress	[0 1]	Low	TRAPMF	[-0.5 -0.25 0.25 0.5]
			Medium	TRAPMF	[0 0.25 0.75 1]
			High	TRAPMF	[0.5 0.75 1.25 1.5]

TABLE 2. Expert knowledge-based rules.

MHP	VHP	VGSR	AGSR	HSCR	Weight	Connection	Stress
High	-	-	-	-	0.3	OR	High
Medium	-	-	-	-	0.3	OR	Medium
Low	-	-	-	Low	0.3	OR	Low
High	-	-	-	High	0.4	AND	High
Medium	-	-	-	Medium	0.5	AND	Medium
Low	-	-	-	Low	0.6	AND	Low
High	-	-	High	High	0.7	AND	High
Low	-	Low	Low	Low	0.8	AND	Low
High	High	High	High	High	1	AND	High
Medium	Medium	Medium	-	Medium	1	AND	Medium
Low	Low	Low	Low	Low	1	AND	Low
-	-	Low	Low	-	0.5	AND	Low
-	Low	Low	-	-	0.1	OR	Low
-	High	High	-	-	0.1	OR	High
-	Low	Low	-	-	0.2	AND	Low
-	High	High	-	-	0.2	AND	High
High	-	-	-	Low	0.2	AND	Medium
-	-	-	-	High	0.1	OR	High
-	-	-	-	Medium	0.2	OR	Medium
-	Medium	Medium	-	-	0.1	OR	Medium
-	Medium	Medium	-	-	0.2	AND	Medium

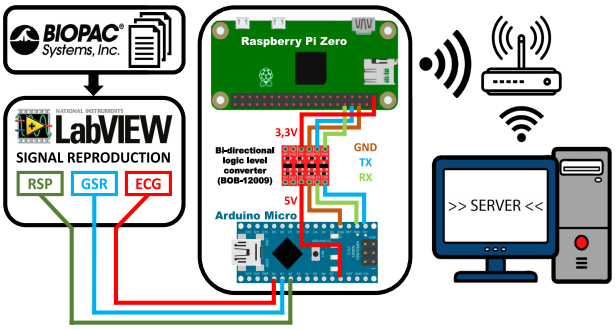

FIGURE 7. Scheme of interconnected signal reproduction, acquisition, processing and server systems.

language, which consists of a set of C/C++ functions that can be called from the code.

An important parameter when acquiring ECG, GSR and RSP is the sampling frequency, which must be high enough so

TABLE 3. Server specifications.

Hardware	- Intel Core duo E8400 @ 3.0GHz - 2 GB RAM - TP-Link WiFi Router (TL-WR841ND)
Software	- Ubuntu server 18.04 - Kubuntu desktop environment
Protocols	- MQTT Broker (Server) version 3.1.1 - SQL server

that important details of the signal are not lost but low enough so that the computational load is not excessive. Considering that the three physiological signals are acquired simultaneously, a frequency that satisfies all sampling requirements is necessary.

According to the literature, GSR provides sufficient information with a minimal sampling frequency of 32 Hz [37]. For ECG, QRS complexes can be detected effectively at 200 Hz [32], [38]. In studies conducted on the RSP, the 0.4-Hz band is commonly applied [4]. According to the Nyquist frequency,

TABLE 4. Results obtained after comparing stress-relaxation level estimation with the labeling performed by UPV/EHU physiology experts on the 42 registers recorded in the experimental stage.

Tape No.	TP	TN	FP	FN	P^+ (%)	Se (%)	$F1^+$ (%)	P^- (%)	Sp (%)	$F1^-$ (%)
1	7	14	0	0	100.00	100.00	100.00	100.00	100.00	100.00
2	9	41	7	0	56.25	100.00	72.00	100.00	85.42	92.13
3	10	39	2	0	83.33	100.00	90.91	100.00	95.12	97.50
4	5	17	0	0	100.00	100.00	100.00	100.00	100.00	100.00
5	11	6	0	0	100.00	100.00	100.00	100.00	100.00	100.00
6	7	28	0	0	100.00	100.00	100.00	100.00	100.00	100.00
7	15	43	0	1	100.00	93.75	96.77	97.73	100.00	98.85
8	14	46	0	1	100.00	93.33	96.55	97.87	100.00	98.92
9	10	55	5	1	66.67	90.91	76.92	98.21	91.67	94.83
10	17	10	6	3	73.91	85.00	79.07	76.92	62.50	68.97
11	13	37	0	0	100.00	100.00	100.00	100.00	100.00	100.00
12	3	12	0	0	100.00	100.00	100.00	100.00	100.00	100.00
13	6	24	0	0	100.00	100.00	100.00	100.00	100.00	100.00
14	9	15	0	1	100.00	90.00	94.74	93.75	100.00	96.77
15	20	18	0	4	100.00	83.33	90.91	81.82	100.00	90.00
16	7	35	6	1	53.85	87.50	66.67	97.22	85.37	90.91
17	20	68	9	0	68.97	100.00	81.63	100.00	88.31	93.79
18	10	20	0	1	100.00	90.91	95.24	95.24	100.00	97.56
19	20	31	0	4	100.00	83.33	90.91	88.57	100.00	93.94
20	7	15	0	2	100.00	77.78	87.50	88.24	100.00	93.75
21	4	33	0	1	100.00	80.00	88.89	97.06	100.00	98.51
22	9	30	3	0	75.00	100.00	85.71	100.00	90.91	95.24
23	8	33	0	1	100.00	88.89	94.12	97.06	100.00	98.51
24	3	4	0	5	100.00	37.50	54.55	44.44	100.00	61.54
25	4	32	0	0	100.00	100.00	100.00	100.00	100.00	100.00
26	6	35	0	1	100.00	85.71	92.31	97.22	100.00	98.59
27	9	32	0	0	100.00	100.00	100.00	100.00	100.00	100.00
28	3	33	0	1	100.00	75.00	85.71	97.06	100.00	98.51
29	5	7	0	0	100.00	100.00	100.00	100.00	100.00	100.00
30	7	36	3	0	70.00	100.00	82.35	100.00	92.31	96.00
31	6	25	1	1	85.71	85.71	85.71	96.15	96.15	96.15
32	7	23	1	1	87.50	87.50	87.50	95.83	95.83	95.83
33	22	33	0	1	100.00	95.65	97.78	97.06	100.00	98.51
34	31	43	2	0	93.94	100.00	96.88	100.00	95.56	97.73
35	12	37	0	0	100.00	100.00	100.00	100.00	100.00	100.00
36	0	16	0	0	-	-	-	100.00	100.00	100.00
37	15	15	0	0	100.00	100.00	100.00	100.00	100.00	100.00
38	6	18	0	1	100.00	85.71	92.31	94.74	100.00	97.30
39	6	14	0	0	100.00	100.00	100.00	100.00	100.00	100.00
40	0	26	0	0	-	-	-	100.00	100.00	100.00
41	15	7	0	1	100.00	93.75	96.77	87.50	100.00	93.33
42	9	21	0	1	100.00	90.00	94.74	95.45	100.00	97.67
Total	**407**	**1127**	**45**	**34**	**90.04**	**92.29**	**91.15**	**97.07**	**96.16**	**96.61**

a sampling frequency greater than 0.8 Hz would be sufficient for RSP; however, in the literature, sampling frequencies up to 4 Hz are used [37]. Based on this information, a frequency of 200 Hz satisfies all the requirements for robust sampling of ECG, GSR and RSP.

2) PROCESSING

According to the computational power requirements for this stage of the implementation, the researchers selected an RPiZ platform due to its small size, computational capacity and low price. The RPiZ is a single-board computer with several inputs and outputs to allow the connection of many peripherals. The RPiZ can run several operating systems (OSs), with the capacity to perform any task expected from a common desktop computer [14], [17]. For this solution, the Raspbian Stretch Lite OS was utilized, which eliminates the interface and focuses the performance on physiological data processing and a wireless server connection. Moreover, the Python programming language, which is fully integrated in all Raspbian OSs and offers a wide set of tools for carrying out different processes, was employed.

RPiZ does not have analog inputs; thus, the data arrive directly through the serial port from the ArdM board. This connection was made using a bidirectional logic-level converter that connects the serial pins of the ArdM (Rx and Tx), which operates at 5 V, with the serial pins in the RPiZ, which operates at 3.3 V. A schematic representation of this connection is shown in Figure 7.

Data received from the serial port are stored in a 20-second sliding window. The window is updated every 5 seconds by discarding the oldest data and stacking new data following the FIFO protocol. Subsequently, parameter extraction and normalization are performed from the physiological registers stored in the sliding window, followed by fuzzy processing, which produces an estimation of the stress-relaxation level, as shown in Figure 8.

TABLE 5. Comparison of stress and relaxation estimation performance represented by *Se* and *Sp*, respectively.

Reference	Se (%)	Sp (%)	Signals	n	HW	P	RT	W/S	Price
Sharawi et al. [39]	60-78	-	ST, GSR	35	Yes	No	Yes	-/-	Not available
Gjoreski et al. [10]	70	-	PPG, ST, GSR, ACC	5	Yes	Yes	Yes	2-20/- min	+1000€
Salai et al. [13]	75	74.2	ECG	5	Yes	Yes	No	560/20 HP	+115€
Kulic and Croft [40]	76	-	ECG, EMG, GSR	8	No	No	No	-/-	No device
Guang-yuan and Min [41]	75-85	-	ECG, EMG, GSR, RSP	1	No	No	No	-/-	No device
Golgouneh and Tarvirdizadeh [11]	81	-	PPG, GSR	16	Yes	Yes	Yes	20/1 sec	+80€
Minguillon et al. [12]	86	-	ECG, EMG, EEG, GSR	10	Yes	Yes	Yes	2/2 sec	Not available
Wagner et al. [42]	79.5-96.6	-	ECG, EMG, GSR, RSP	1	No	No	No	2/- min	No device
Cai and Lin [43]	85-96	-	BVP, ST, GSR, RSP	-	Yes	No	No	-/-	Not available
Han et al. [6]	94	94	ECG, RSP	39	No	No	No	1/1 min	No device
Healey and Picard [28]	97.4	-	ECG, EMG, GSR, RSP	24	No	No	Yes	5/- min	No device
Zalabarria et al. [17]	63.95	98.55	ECG, GSR	42	Yes	Yes	Yes	20/5 sec	42€
Proposed	**92.29**	**96.16**	**ECG, GSR, RSP**	**42**	Yes	Yes	Yes	20/5 sec	42€

TABLE 6. Processing times of the proposed algorithm on the Raspberry Pi board (one core).

Device	Process	Mean (ms)	Std (ms)	max (ms)
Arduino	**Acquisition**	**0.937/cycle**	**0.009**	**5.0/cycle**
Raspberry	ECG	2411.139	79.836	
	GSR	3.604	0.066	
	RSP	1109.058	7.804	
	Normalization	0.072	0.007	
	Fuzzy model	102.787	23.110	
	Total RPiZ	**3626.662**	**91.575**	**5000.0**

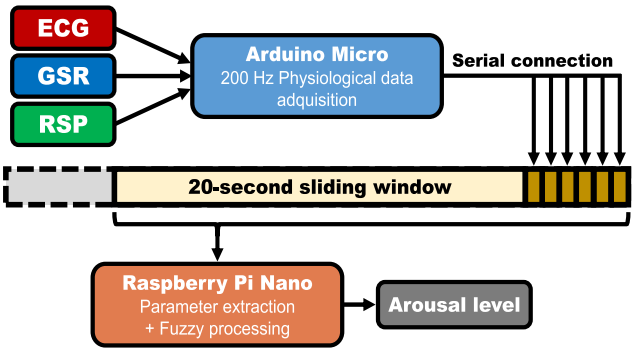

FIGURE 8. Schematic representation of the acquisition, 20-second sliding window generation and arousal level estimation.

3) SERVING

To make the data available remotely, an IoT-based solution is proposed. A widely adopted ISO standard (ISO/IEC PRF 20922) message queuing telemetry transport (MQTT) protocol is deployed. This protocol is based on a publish/subscribe model, where the device publishes the captured data, and the server (also known as a broker) is used for this publication so it can be stored in a database. The device is connected to the server via Wi-Fi to simulate a real use case.

A low-performance PC is employed as the server, which demonstrates that the proposed work can be implemented in a wide range of products. The server specifications are detailed in Table 3.

4) "HUMAN IN THE LOOP"

For system validation, the "human in the loop" configuration was applied. This topology reproduces previously acquired physiological signals to feed the hardware system to be tested. In this way, a person does not need to be connected to the system, the testing and validation stages are simplified, and the benefits of using real physiological signals rather than simulated ideal signals are realized. In this case, the reproduced signals corresponded to the signals that had been previously collected in the experiments using BIOPAC MP36. These signals were reproduced using a National Instruments Single-Board RIO 9631 at the same sampling frequency and resolution with which the original signals had been captured with BIOPAC MP36. Therefore, the quality of the reproduced signals was the same as the original capture of the BIOPAC device, which is considered to be the gold standard in medical devices.

III. RESULTS AND DISCUSSION

To assess the effectiveness of the proposed method for the estimation of stress and relaxation, the results are compared with the labels of UPV/EHU physiology experts. Table 4 presents the results obtained for the 42 registers recorded during the experimental stage. The true-positive (TP), true-negative (TN), false-positive (FP) and false-negative (FN) results were applied to calculate the positive predictivity (16), negative predictivity (17), sensitivity (18), specificity (19), positive F1 score (20) and negative F1 score (21). Positive and negative refer to the results obtained according to the predictions of stress and relaxation, respectively.

$$P^{+} = \frac{TP}{TP + FP} \quad (\%) \tag{16}$$

$$P^{-} = \frac{TN}{TN + FN} \quad (\%) \tag{17}$$

$$Se = \frac{TP}{TP + FN} \quad (\%) \tag{18}$$

$$Sp = \frac{TN}{TN + FP} \quad (\%) \tag{19}$$

$$F1^{+} = 2 \cdot \frac{P^{+} \cdot Se}{P^{+} + Se} \quad (\%) \tag{20}$$

$$F1^{-} = 2 \cdot \frac{P^{-} \cdot Sp}{P^{-} + Sp} \quad (\%) \tag{21}$$

To compare the stress and relaxation level estimates (ranging between 0 and 1) with the binary format labels, error metrics are defined as follows: TP corresponds to a real state of stress in which the algorithm detects a stress level > 0.5, TN corresponds to a real state of relaxation in which the algorithm detects a stress level ≤ 0.5, FP corresponds to a real state of relaxation in which the algorithm detects a stress level > 0.5, and FN corresponds to a real state of stress in which the algorithm detects a stress level ≤ 0.5.

Results with a high percentage of success in the detection of stress and relaxation were achieved with F1 scores of 91.15% and 96.61%. Relaxation has a higher success rate, as indicated by the negative F1 score. This higher rate is usually due to the ease of identifying relaxation by the lack of activation of the sympathetic nervous system, resulting in more stable parameter values. Moreover, identifying stress, which is measured by the positive F1 score, is more difficult because quantifying the exact level of arousal in different stressful situations is challenging.

Some records of Table 4, such as 2, 9, 10, 16 and 24, are below the average. In a further analysis of these cases, normalization was corrupted due to outlier values, which caused a loss of effectiveness of the MFs of the fuzzy algorithm and an increase in FP and FN.

Table 5 compares the performance of the proposed algorithm with well-known studies, including the predecessor of this work [17]. Furthermore, this work compares the current system with its preceding version using the same database obtained in the experimental stage, which enables a fair comparison. A graphical representation of the comparison is shown in Figure 9.

Table 5 also includes information on whether the solution proposed by each author is integrated into a hardware device (HW), if the device is portable (P) and if the execution is carried out in real time (RT). The population size (n), acquired physiological signals, size of the sliding window/step (W/S) and price of the device have also been indicated. The price of the proposed prototype is the sum of the ArdM and RPiZ boards since the remaining devices have only been employed in the experimental stage and in the preliminary development stage: BIOPAC MP36 for the acquisition and generation of the database, which is utilized for the development of the software, and the National Instruments Single-Board RIO 9631, which is employed to test the final prototype for reproducing previously acquired physiological records.

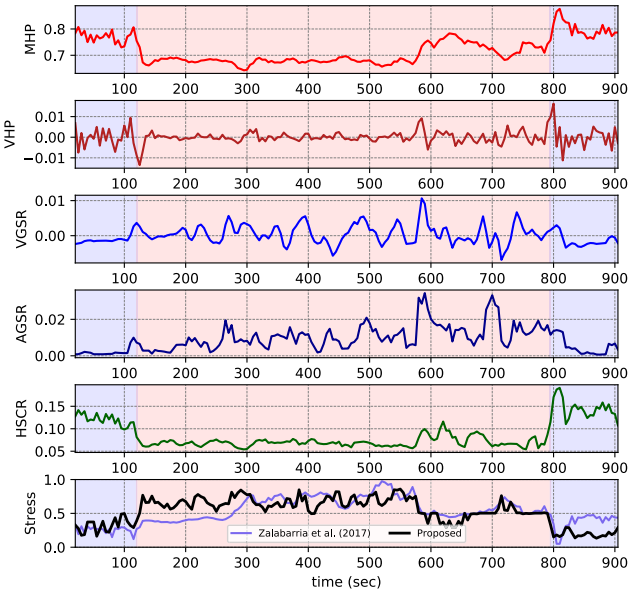

FIGURE 9. Graphical representation of stress level estimation according to different combinations of parameter values.

The RSP signal was initially studied due to its influence on both sweating and heart rhythm. The results support the fact that the RSP is closely related to variations in the sympathetic and parasympathetic nervous systems [4], [24]. One of the main contributions of this work with respect to the proposals in the literature is the influence of respiratory action on the improvement of the obtained results, as shown in Table 5. In previous works, such as Han *et al.* [6], the use of RSP cycle time and amplitude is proposed. This work has improved the results achieved in Zalabaria *et al.* [17] by using the standard deviation of the RSP frequency correlation as a reliable stress and relaxation level estimator.

One of the main problems with the use of the raw GSR signal is the difference in magnitude at different stages of relaxation over a period. This phenomenon is reflected in the purple stress line of Figure 9, where the level of stress in the final relaxation stage is higher than that in the initial stage due to the accumulated humidity during the experiment. This proposal has solved this problem by discarding the use of the raw GSR signal as an input parameter, which eliminates the influence of the GSR offset. Instead, a new GSR-derived parameter, i.e., AGSR, was utilized and further improved the results.

In terms of hardware implementation, the algorithm must be within established performance ranges to offer a real perspective for medical and commercial use. Therefore, to carry out data acquisition and transmission in real time at 200 Hz, the ArdM must execute each sampling and data transmission cycle in less than 1/200 Hz = 5 ms. Moreover, the step of the sliding window has been set to 5 seconds; this value is the maximum time available for processing the current window until the next window is available. Table 6 presents the average times (in milliseconds) measured for each of

the tasks executed in each of the devices with the standard deviation (std) due to the concurrent execution of other OS processes.

In the acquisition carried out by the ArdM and the processing executed in the RPiZ, the measured times do not reach the maximum threshold, which leaves a considerable margin of safety and ensures robust real-time execution of the proposed algorithm.

The low cost and performance of the components employed for the proposed method render commercial implementation possible. Thus, the developed algorithm could be successfully implemented in an embedded device that satisfies the safety and stability requirements for a real medical device.

IV. CONCLUSION

This paper proposes a novel development for stress and relaxation level estimation, which is calculated by using a computationally efficient model. The developed algorithm consists of rule-based fuzzy logic processing, where the output is successfully modeled using parameters extracted from the electrocardiogram, galvanic skin response and breath signals. In addition, all the code is efficiently implemented in a low-cost hardware prototype.

The algorithm was tested on registers acquired in stressful and relaxing conditions. The use of reliable parameters derived from the breath and galvanic skin response signals has helped to improve the previous results. As a result, the accuracy obtained in previous works has been improved, which provides a robust estimation of stress and relaxation with F1 scores of 91.15% and 96.61%, respectively.

All the work was then implemented in a prototype that was tested in real time, which demonstrates the feasibility of connecting several low-cost devices for robust physiological data acquisition, processing and wireless storage of results in a cloud server.

This work improves the proposals in the literature via portable, low-cost, real-time execution and quality results. We believe that this proposal represents a first step for the development of an embedded low-cost device for medical and commercial use.

ACKNOWLEDGMENT

This work was performed with the support of the University of the Basque Country (UPV/EHU) and the Intelligent Control Research Group of the UPV/EHU, to which the authors are very grateful.

REFERENCES

[1] W. B. Cannon, "Stresses and strains of homeostasis," *Amer. J. Med. Sci.*, vol. 189, no. 1, pp. 13–14, Jan. 1935.

[2] G. Fink, *Stress: Concepts, Cognition, Emotion, and Behavior: Handbook of Stress*. Amsterdam, The Netherlands: Elsevier, 2016.

[3] H. Selye, *Stress in Health and Disease*. Oxford, U.K.: Butterworth-Heinemann, 2013.

[4] J. T. Cacioppo, L. G. Tassinary, and G. Berntson, *Handbook of Psychophysiology*. Cambridge, U.K.: Cambridge Univ. Press, 2007.

[5] C. R. Snyder and S. J. Lopez, *Handbook of Positive Psychology*. London, U.K.: Oxford Univ. Press, Dec. 2001.

[6] L. Han, Q. Zhang, X. Chen, Q. Zhan, T. Yang, and Z. Zhao, "Detecting work-related stress with a wearable device," *Comput. Ind.*, vol. 90, pp. 42–49, Sep. 2017.

[7] N. Sharma and T. Gedeon, "Modeling a stress signal," *Appl. Soft Comput.*, vol. 14, pp. 53–61, Jan. 2014.

[8] *Safer and Healthier Work for All—Modernisation of the EU Occupational Safety and Health Legislation and Policy*, Eur. Commission, Brussels, Belgium, Jan. 2017.

[9] M. E. P. Seligman and M. Csikszentmihalyi, *Positive Psychology: An Introduction*. Dordrecht, The Netherlands: Springer, 2014, pp. 279–298.

[10] M. Gjoreski, M. Luštrek, M. Gams, and H. Gjoreski, "Monitoring stress with a wrist device using context," *J. Biomed. Inform.*, vol. 73, pp. 159–170, Sep. 2017.

[11] A. Golgouneh and B. Tarvirdizadeh, "Fabrication of a portable device for stress monitoring using wearable sensors and soft computing algorithms," *Neural Comput. Appl.*, Jun. 2019.

[12] J. Minguillon, E. Perez, M. Lopez-Gordo, F. Pelayo, and M. Sanchez-Carrion, "Portable system for real-time detection of stress level," *Sensors*, vol. 18, no. 8, p. 2504, Aug. 2018.

[13] M. Salai, I. Vassányi, and I. Kósa, "Stress detection using low cost heart rate sensors," *J. Healthcare Eng.*, vol. 2016, pp. 1–13, Jun. 2016.

[14] F. Slauddin and T. R. Rahman, "A fuzzy based low-cost monitoring module built with raspberry Pi–Python–Java architecture," in *Proc. Int. Conf. Smart Sensors Appl. (ICSSA)*, 2015, pp. 1–6.

[15] L. J. V. Escobar and S. A. Salinas, "E-health prototype system for cardiac telemonitoring," in *Proc. 38th Annu. Int. Conf. IEEE Eng. Med. Biol. Soc. (EMBC)*, Aug. 2016, pp. 4399–4402.

[16] C. O. Fernandes, C. J. P. de Lucena, C. A. P. de Lucena, and B. A. de Azevedo, "Enabling a smart and distributed communication infrastructure in healthcare," in *Innovation in Medicine and Healthcare*. Cham, Switzerland: Springer, 2016, pp. 435–446.

[17] U. Zalabarria, E. Irigoyen, R. Martínez, and J. Arechalde, "Acquisition and fuzzy processing of physiological signals to obtain human stress level using low cost portable hardware," in *Proc. Int. Joint Conf. SOCO-CISIS-ICEUTE*. León, Spain: Springer, Aug./Sep. 2017, pp. 68–78.

[18] M. U. H. Al Rasyid, F. A. Saputra, and A. Christian, "Implementation of blood glucose levels monitoring system based on wireless body area network," in *Proc. IEEE Int. Conf. Consum. Electron.-Taiwan (ICCE-TW)*, May 2016, pp. 1–2.

[19] Y. Ungson, M. A. Reyna, and M. E. Bravo-Zanoguera, "Development of an ambulatory ECG system based on Arduino and mobile telephony for wireless transmission," in *Proc. Pan Amer. Health Care Exchanges (PAHCE)*, Apr. 2014, pp. 1–5.

[20] E. Montón, J. F. Hernandez, J. M. Blasco, T. Hervé, J. Micallef, I. Grech, A. Brincat, and V. Traver, "Body area network for wireless patient monitoring," *IET Commun.*, vol. 2, no. 2, pp. 215–222, 2008.

[21] E. Jovanov, A. O. D. Lords, D. Raskovic, P. G. Cox, R. Adhami, and F. Andrasik, "Stress monitoring using a distributed wireless intelligent sensor system," *IEEE Eng. Med. Biol. Mag.*, vol. 22, no. 3, pp. 49–55, May 2003.

[22] J. J. Gross and R. W. Levenson, "Emotion elicitation using films," *Cognition Emotion*, vol. 9, no. 1, pp. 87–108, Jan. 1995.

[23] R. Martínez, E. Irigoyen, N. Asla, I. Escobes, and A. Arruti, "First results in modelling stress situations by analysing physiological human signals," in *Proc. IADIS Int. Conf. e-Health*, M. Macedo, Ed., Jul. 2012, pp. 171–175.

[24] S. D. Kreibig, "Autonomic nervous system activity in emotion: A review," *Biol. Psychol.*, vol. 84, no. 3, pp. 394–421, Jul. 2010.

[25] E. M. Sokhadze, "Effects of music on the recovery of autonomic and electrocortical activity after stress induced by aversive visual stimuli," *Appl. Psychophysiol. Biofeedback*, vol. 32, no. 1, pp. 31–50, Mar. 2007.

[26] A. Ezeiza, N. Garay-Vitoria, K. L. de Ipiña, and A. Soraluze, "Ethical issues on the design of assistive technology for people with mental disabilities," in *Proc. Int. Conf. Ethics Hum. Values Eng.*, Mar. 2008, pp. 75–84.

[27] A. Salazar-Ramirez, E. Irigoyen, R. Martinez, and U. Zalabarria, "An enhanced fuzzy algorithm based on advanced signal processing for identification of stress," *Neurocomputing*, vol. 271, pp. 48–57, Jan. 2018.

[28] J. A. Healey and R. W. Picard, "Detecting stress during real-world driving tasks using physiological sensors," *IEEE Trans. Intell. Transp. Syst.*, vol. 6, no. 2, pp. 156–166, Jun. 2005.

[29] A. Schäfer and J. Vagedes, "How accurate is pulse rate variability as an estimate of heart rate variability?: A review on studies comparing photoplethysmographic technology with an electrocardiogram," *Int. J. Cardiol.*, vol. 166, no. 1, pp. 15–29, 2013.
[30] F. Shaffer, R. McCraty, and C. L. Zerr, "A healthy heart is not a metronome: An integrative review of the heart's anatomy and heart rate variability," *Frontiers Psychol.*, vol. 5, p. 1040, Sep. 2014.
[31] S. Laborde, E. Mosley, and J. F. Thayer, "Heart rate variability and cardiac vagal tone in psychophysiological research–recommendations for experiment planning, data analysis, and data reporting," *Frontiers Psychol.*, vol. 8, p. 213, Feb. 2017.
[32] U. Zalabarria, E. Irigoyen, R. Martinez, and A. Lowe, "Online robust R-peaks detection in noisy electrocardiograms using a novel iterative smart processing algorithm," *Appl. Math. Comput.*, vol. 369, Mar. 2020, Art. no. 124839.
[33] A. de Santos Sierra, C. S. Ávila, J. G. Casanova, and G. B. del Pozo, "A stress-detection system based on physiological signals and fuzzy logic," *IEEE Trans. Ind. Electron.*, vol. 58, no. 10, pp. 4857–4865, Oct. 2011.
[34] R. Martinez, A. Salazar-Ramirez, A. Arruti, E. Irigoyen, J. I. Martin, and J. Muguerza, "A self-paced relaxation response detection system based on galvanic skin response analysis," *IEEE Access*, vol. 7, pp. 43730–43741, 2019.
[35] P. Grossman and E. W. Taylor, "Toward understanding respiratory sinus arrhythmia: Relations to cardiac vagal tone, evolution and biobehavioral functions," *Biol. Psychol.*, vol. 74, no. 2, pp. 263–285, Feb. 2007.
[36] U. Zalabarria, E. Irigoyen, R. Martínez, and A. Salazar-Ramirez, "Detection of stress level and phases by advanced physiological signal processing based on fuzzy logic," in *Proc. Int. Conf. Eur. Trans. Educ.* Cham, Switzerland: Springer, 2016, pp. 301–312.
[37] C.-Y. Chang, J.-Y. Zheng, C.-J. Wang, and P.-C. Chung, "Application of support vector regression for phyciological emotion recognition," in *Proc. Int. Comput. Symp. (ICS)*, Dec. 2010, pp. 12–17.
[38] P. Hamilton, "Open source ECG analysis," in *Proc. Comput. Cardiol.*, Sep. 2002, pp. 101–104.
[39] M. S. Sharawi, M. Shibli, and M. I. Sharawi, "Design and implementation of a human stress detection system: A biomechanics approach," in *Proc. 5th Int. Symp. Mechatronics Appl.*, May 2008, pp. 1–5.
[40] D. Kulic and E. Croft, "Anxiety detection during human-robot interaction," in *Proc. IEEE/RSJ Int. Conf. Intell. Robots Syst.*, Aug. 2005, pp. 616–621.
[41] L. Guang-Yuan and H. Min, "Emotion recognition of physiological signals based on adaptive hierarchical genetic algorithm," in *Proc. WRI World Congr. Comput. Sci. Inf. Eng.*, vol. 4, Mar. 2009, pp. 670–674.
[42] J. Wagner, J. Kim, and E. Andre, "From physiological signals to emotions: Implementing and comparing selected methods for feature extraction and classification," in *Proc. IEEE Int. Conf. Multimedia Expo*, Jul. 2005, pp. 940–943.
[43] H. Cai and Y. Lin, "An experiment to non-intrusively collect physiological parameters towards driver state detection," SAE Tech. Paper 2007-01-0403, SAE International, Apr. 2007.

UNAI ZALABARRIA received the bachelor's degree in industrial electronics and automation engineering and the M.Eng. degree in control engineering, automation and robotics from the University of the Basque Country (UPV/EHU), in 2014 and 2016, respectively, where he is currently pursuing the Ph.D. degree with the Systems Engineering and Automation Department. He is also involved in biotechnology research with the Intelligent Control Research Group (GICI), Systems Engineering and Automation Department, UPV/EHU.

ELOY IRIGOYEN (Member, IEEE) received the M.Eng. degree in electrical engineering from the University of the Basque Country (UPV/EHU), in 1992, and the Ph.D. degree in industrial engineering from the Public University of Navarre, in 2003. He has been a Lecturer with the Department of Systems Engineering and Automation, UPV/EHU, since 2001. He has also been an Assistant Lecturer with the Public University of Navarre and the University of Deusto. He is currently leading and managing the Intelligent Control Research Group, UPV/EHU. His main research interests are related to intelligent control and biomedical engineering.

RAQUEL MARTINEZ received the M.Eng. degree in electronic and automation engineering and the Ph.D. degree in automation, robotics and control from the University of the Basque Country, in 2003 and 2016, respectively. She has been a Lecturer with the Department of Systems Engineering and Automation, University of the Basque Country, since 2005. She was the director of three bioelectronic supplementary university modules, from 2014 to 2015. She is currently a Researcher with the Intelligent Control Research Group (GICI), University of the Basque Country.

MIKEL LARREA received the M.Eng. degree in systems engineering and automation and the Ph.D. degree in systems engineering and automation from the University of the Basque Country (UPV/EHU), in 2006 and 2014, respectively. He is currently working as an Assistant Professor with the Faculty of Engineering. His main research interests are related to neural network learning and applications and intelligent control.

ASIER SALAZAR-RAMIREZ received the Engineering degree in electronic engineering from Mondragon University, in 2012, and the master's degree in robotics, automation and control engineering from the University of the Basque Country (UPV/EHU), in 2013. He is currently pursuing the Ph.D. degree with ALDAPA. He is also a Researcher with ALDAPA and GICI Research Groups, UPV/EHU. He is also involved in physiological computing research at ALDAPA.